MIXED SUSPENSION - MIXED PRODUCT REMOVAL CRYSTALLIZATION KINETICS: EFFECT OF THE METHOD OF SUPERSATURATION GENERATION

Stanislav ŽÁČEK[a], Jaroslav NÝVLT[a] and John William MULLIN[b]

[a] *Institute of Inorganic Chemistry, Czechoslovak Academy of Sciences, Majakovského 24, Prague 6, Czechoslovakia and*

[b] *Department of Chemical and Biochemical Engineering, University College London, Torrington Place, London WC1E 7JE, Great Britain*

Received December 16th, 1985

Three methods of continuous crystallization of potassium aluminium sulphate have been compared: crystallization by cooling, precipitation from solutions of component salts (potassium sulphate and aluminium sulphate) and salting-out with ethanol.

Crystal size distribution of the products has been used to obtain crystallization kinetic data in two parallel ways, *viz.* using the concept of population balance and that of mass oversize distribution, both of which led to similar conclusions. The results of cooling and precipitation are comparable, but crystallization by salting-out with ethanol leads to smaller crystals and the results strongly depend on the alcohol concentration, which can be explained by the influence of micromixing.

The knowledge of kinetic data of crystallization is necessary for design of crystallizers as the kinetics determines the size of equipment. Continuous laboratory experiments, which are widely used in the investigation of industrial crystallization processes, have a number of advantages. Under certain conditions (*e.g.* steady state and representative product removal) it is possible to obtain information on both apparent nucleation kinetics and the growth kinetics from the same experiment.

In general, the nucleation and growth rates depend, among other variables, on the supersaturation which can be created by different methods, *e.g.* by cooling, evaporation, precipitation or salting-out. From the strictly theoretical point of view, the supersaturation is always the same, independent on the crystallization mode. Experimental data investigating the effect of the supersaturation creation method on resulting kinetics are extremely sporadic, however.

The aim of this paper is to compare three different ways of producing supersaturation in a continuous laboratory crystallizer using potash alum as a working system: (i) precipitation from component salts, (ii) cooling, (iii) salting-out with ethanol. The effect of above methods on product crystal size distribution and on resulting kinetic data is presented.

THEORETICAL

It is widely accepted that reliable kinetic data for the design of crystallizers can be obtained from the mixed suspension–mixed product removal (MSMPR) crystallizer. Two methods I and II were used for the evaluation of sieve analysis data. In the first, the measured crystal size distribution was converted to number (or population) density, n,

(I) $$n = \frac{m_c(L_1, L_2)}{\alpha \varrho_c \bar{L}_{1,2}^3 \Delta L} \qquad (1)$$

as a function of crystal size, L, and plotted as $\ln n$ against L as suggested by the MSMPR population density balance[1]

(I, II) $$n = n^0 \exp(-L/\dot{L}\bar{t}_1). \qquad (2)$$

From such population density plots (Fig. 1) the slope $= -1/\dot{L}\bar{t}_1$ can be used to calculate the crystal growth rate, $\dot{L}$, while the value of n^0, given by the intercept of the line at $L = 0$, is a measure of the apparent nucleation rate, $\dot{N}_N$, since it can be shown that

(I, II) $$\dot{N}_N = n^0 \dot{L}. \qquad (3)$$

A typical population density plot is shown in Fig. 1. From the best straight line drawn through the points the values of $\dot{L}$, n^0 and hence $\dot{N}_N$ can be thus determined using Eqs (*2*) and (*3*).

The main disadvantage of this method applied to mass distribution data lies[2] in the necessity of converting the mass distribution of crystals, as obtained from the sieve analysis, into the number distribution of crystals and that of population densities, n (Eq. (*1*)). This source of errors may be overcome using the theoretical mass distribution of product crystals which has been derived using (Eq. (*2*) (see Appendix)).

(II) $$M(L) = 100(1 + z + z^2/2 + z^3/6)\exp(-z), \qquad (4)$$

where the dimensionless crystal size is

$$z = L/\dot{L}\bar{t}_1 = 3L/\bar{L}. \qquad (5)$$

From the linear plot (Fig. 2) of values z as obtained from Eq. (*4*), calculated from the corresponding oversize fraction $M(L)$ against the sieve aperture L, the mean size of crystal $\bar{L}$ is determined for $z(\bar{L}) = 3$ and converted into kinetic data for growth rate

(II) $$\dot{L} = \bar{L}/3\bar{t}_1 \qquad (6)$$

and for nucleation rate

$$\text{(II)} \qquad \dot{N}_N = \frac{27 m_c \dot{L}}{2\alpha \varrho_c \bar{L}^4}. \tag{7}$$

The determination of the value of g/n is accomplished in the first case using plot of long $\dot{N}_N$ *vs* log $\dot{L}$ (or log n^0 *vs* log $\dot{L}$) according to the equations

$$\text{(I)} \qquad \dot{N}_N = \text{const.}\ \dot{L}^{n/g} \tag{8}$$

or

$$\text{(I)} \qquad n^0 = \text{const.}\ \dot{L}^{(n/g-1)} \tag{9}$$

(Fig. 3).

In the second case, the plot of log $\bar{L}$ *vs* log $\dot{m}_c$ according to the equation

$$\text{(II)} \qquad \frac{\mathrm{d} \log \bar{L}}{\mathrm{d} \log \dot{m}_c} = \frac{g/n - 1}{1 + 3g/n} \tag{10}$$

is used (Fig. 4) and from the slope of the log $\bar{L}$ *vs* log $\dot{m}_c$ line, equal to $(g/n - 1)/(1 + 3g/n)$, the value of g/n is calculated.

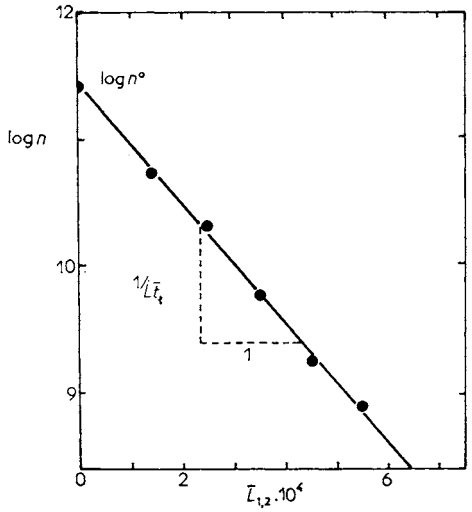

FIG. 1
Population density plot

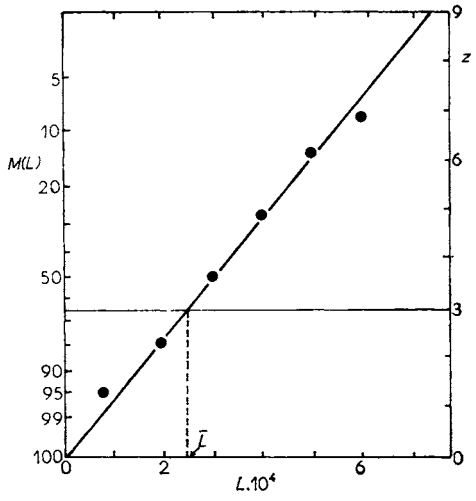

FIG. 2
Mass distribution plot in coordinates $z-L$

Further treatment of data can be made using the design equation

$$\bar{L}^{1+3g/n} = 3B_N m_c^{1-cg/n} \dot{m}_c^{g/n-1} \qquad (11)$$

also derived in the Appendix, where the relative kinetic exponent g/n, the exponent of secondary nucleation c and the system constant B_N are used for the characterization of kinetics.

It has been suggested[2] that the first method is suitable for experiments where the number distribution of crystals is determined directly while the second method suits better for treatment of weight distributions (sieve analysis data).

EXPERIMENTAL

All experiments were carried out in a 400 ml MSMPR crystallizer[3,4]. In the first series, potash alum was precipitated from its components (potassium and aluminium sulphates) using stock solution concentration in the range 0·4—0·6 mol l^{-1}. In the second series, crystallization was carried out by cooling of potash alum solutions saturated at 35 and 45°C, respectively, down to 25°C. In the third series, supersaturation was created by salting-out, *i.e.* by mixing potash alum solutions saturated at 25°C with aqueous ethanol of concentrations 50, 70, and 90% C_2H_5OH, respectively. All experiments were carried out under the same conditions of temperature 25°C and agitation 700 r.p.m. The mean retention time was in the range 800—4 500 s and crystal slurry

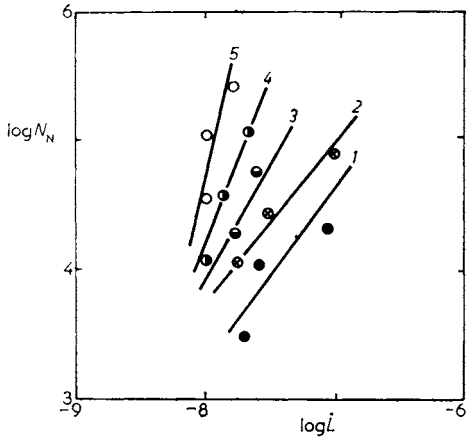

FIG. 3

Plot of nucleation *vs* growth rate, *1* — ● cooling, *2* — ⊗ precipitation, *3* — ◒ salting out by 50% ethanol, *4* — ◑ salting out by 70% ethanole, *5* — ○ salting out by 90% ethanol

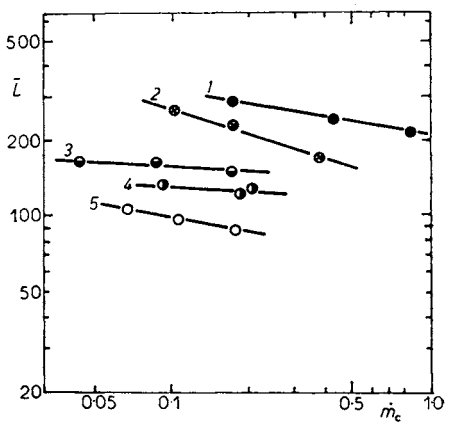

FIG. 4

Plot of mean crystal size *vs* production rate Description of lines the same as in Fig. 3

concentration, m_c, in the range 0·05—0·35 kg hydrate/kg free water. CSD determinations were made using standard sieves in the range 0·08—1·0 mm.

TABLE I
Evaluation of individual experiments

$\bar{t}_1$	m_c	$\bar{L} \cdot 10^3$	$\dot{L} \cdot 10^8$		$n^0 \cdot 10^{-11}$	$\dot{N}_N$	
			Eq. (4)	Eq. (5)	Eq. (5)	Eq. (3)	Eq. (6)
Cooling: T_{sat} = 35°C							
1 110	0·059	0·306	9·18	8·23	1·875	10 070	15 431
2 028	0·065	0·342	5·62	5·42	0·769	4 349	4 177
3 180	0·057	0·322	3·36	3·61	0·512	2 914	1 848
Cooling: T_{sat} = 40°C							
972	0·100	0·282	9·67	8·86	2·620	24 903	11 480
2 028	0·100	0·269	4·38	4·64	2·761	13 751	12 806
3 180	0·089	0·328	3·42	3·23	1·370	4 305	4 425
Precipitation: 0·4 mol l^{-1}							
840	0·060	0·235	9·28	9·01	3·252	29 877	29 282
1 680	0·065	0·257	5·05	4·64	2·630	12 373	12 203
3 702	0·060	0·297	2·67	2·66	1·193	3 358	3 165
Precipitation: 0·6 mol l^{-1}							
798	0·188	0·245	10·10	9·62	9·042	86 963	89 676
1 680	0·195	0·250	4·94	4·74	4·740	40 323	42 849
3 702	0·176	0·271	2·43	2·91	2·630	12 967	7 653
Salting-out: 50% C_2H_5OH							
1 200	0·058	0·154	4·25	4·76	1·221	70 600	58 070
2 280	0·055	0·181	2·63	2·58	0·921	22 083	23 760
4 524	0·055	0·166	1·21	1·31	0·828	14 427	10 846
Salting-out: 70% C_2H_5OH							
1 200	0·068	0·124	3·41	3·55	4·320	161 339	153 360
1 200	0·062	0·120	3·33	3·59	3·851	162 310	138 215
2 400	0·062	0·133	1·83	1·82	3·502	59 607	63 700
Salting-out: 90% C_2H_5OH							
1 200	0·062	0·086	2·33	2·49	18·706	443 799	465 630
2 400	0·068	0·097	1·33	1·30	13·501	168 523	175 500
3 600	0·068	0·121	1·11	1·18	4·85	57 880	57 230

The values of mean crystal size, L, linear crystal growth rate, $\dot{L}$, nucleation rate, $\dot{N}_N$, and nuclei population density, n^0, for a given method of supersaturation creation and for both ways of evaluation are summarised in Table I for individual experimental conditions such as mean retention time, $\bar{t}_I$, and crystal slurry concentration, m_c. Examples of the population density plot and of the mass distribution plot are shown in Fig. 1 and Fig. 2, respectively.

The values of g/n, calculated using Eqs. (*9*) and (*10*), values of the secondary nucleation exponent, c, and the kinetic constant, B_N as evaluated from Eq. (*11*), are presented in Table II. Typical plots are shown in Fig. 3 and Fig. 4. Values of L, shown also in Table II, were back calculated for equal suspension concentration, m_c, and equal mean retention times, $\bar{t}_I$, using Eq. (*11*). These values demonstrate clearly the effect of the method by which supersaturation is created.

DISCUSSION AND CONCLUSIONS

As could be expected (see Table I), the mean crystal size depends on the mean retention time of solution: the longer the retention time, the larger are the crystals (Fig. 5).

TABLE II
Kinetic data

Mode	Cooling	Precipitation	Salting-out		
			50%	70%	90%
g/n, Eq. (*8*)	0·777	0·676	0·810	0·668	0·372
g/n, Eq. (*9*)	0·561	0·506	0·772	0·651	0·425
c	2	1	0	0	0
B_N	$1{\cdot}698 \cdot 10^{-14}$	$4{\cdot}104 \cdot 10^{-13}$	$8{\cdot}886 \cdot 10^{-13}$	$3{\cdot}516 \cdot 10^{-13}$	$2{\cdot}548 \cdot 10^{-11}$
$\bar{L}$	$2{\cdot}94 \cdot 10^{-4}$	$2{\cdot}68 \cdot 10^{-4}$	$1{\cdot}92 \cdot 10^{-4}$	$1{\cdot}46 \cdot 10^{-4}$	$1{\cdot}11 \cdot 10^{-4}$

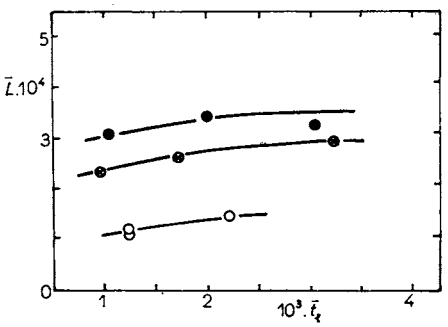

FIG. 5
Plot of mean crysal size *vs* mean retention time Description of curves as in Fig. 3

However, the crystal size depends also on the way in which supersaturation is created: The biggest crystals were obtained by cooling and precipitation, smallest by salting-out. In the latter case the crystal size depends on the alcohol concentration – for diluted precipitant the results are better. Apparently, micromixing plays an important role.

With the increase of crystal size, secondary nucleation proceeds with various mechanisms, as indicated by the exponent of secondary nucleation, c (see Table II): in salting-out, the adsorbed layer mechanism predominates; in precipitation, crystal-impeller collisions seem to be important; and in cooling, crystal-crystal collisions are rate-determining.

Kinetic data obtained in this paper (Figs 3, 4) are similar to those published by other authors[5,6]. In spite of simplifications introduced in the theoretical treatment, is it shown that both theoretical approaches viz the crystal number population balance (I) and the crystal mass distribution method (II), lead to similar results, although the difference in the value of g/n is not negligible.

APPENDIX

Derivation of basic equations used in the theoretical part of this paper:

The mass of crystals in a unit amount of suspension in the crystallizer is

$$m_c = \int_0^\infty \alpha \varrho_c L^3 n(L)\, \mathrm{d}L \qquad (A1)$$

which gives for the distribution function $n(L)$ defined by Eq. (2)

$$m_c = 6\alpha \varrho_c n^0 (\dot{L}\bar{t}_1)^4 \,. \qquad (A2)$$

In a similar way, it holds for the mass of crystals larger than a given size L

$$m_c(L) = \int_L^\infty \alpha \varrho_c L^3 n(L)\, \mathrm{d}L =$$

$$= 6\alpha \varrho_c n^0 (\dot{L}\bar{t}_1)^4 (1 + z + z^2/2 + z^3/6) \exp(-z) \,. \qquad (A3)$$

It follows for the oversize fraction

$$M(L) = 100 m_c(L)/m_c = 100(1 + z + z^2/2 + z^3/6) \exp(-z) \qquad (A4)$$

which is identical with Eq. (4). The inflection point of the $M(L)$ *vs* z curve (maximum of the differential distribution of crystals) corresponds to the condition

$$\mathrm{d}^2 M(L)/\mathrm{d}z^2 = 0 \qquad (A5)$$

with the solution $z(\bar{L}) = 3$, from which then result Eqs. (5) and (6). Hence

$$\bar{L} = 3\dot{L}\bar{t}_1 \,. \qquad (A6)$$

Substitution of this equation into Eq. (*A2*) gives

$$n^0 = 27m_c/2\alpha\varrho_c\bar{L}^4 \qquad (A7)$$

and insertion into Eq. (*3*) leads directly to Eq. (*7*) for the nucleation rate.

The nucleation rate is very often expressed by the power law equation

$$\dot{N}_N = k_N m_c^c \, \Delta w^n \qquad (A8)$$

and similarly the growth rate

$$\dot{L} = k_G\beta/(3\alpha\varrho_c) \, \Delta w^g \, . \qquad (A9)$$

Eliminating the unknown supersaturation, Δw, from these equations, we can write

$$\dot{N}_N = k_N m_c^c (3\alpha\varrho_c/k_G\beta)^{g/n} \, \dot{L}^{n/g} \qquad (A10)$$

which may be compared with Eq. (*8*).

Using Eq. (A6) and Eq. (*3*), we can transform Eq. (*A2*) into

$$m_c = \frac{2}{9}\alpha\varrho_c\dot{N}_N\bar{L}^3\bar{t}_1 \qquad (A11)$$

or, because it holds

$$m_c/\bar{t}_1 = \dot{m}_c \qquad (A12)$$

$$\bar{L}^3 = 4{\cdot}5/\alpha\varrho_c\dot{N}_N \, \dot{m}_c \, . \qquad (A13)$$

Substitution of $\dot{N}_N$ from Eq. (*A10*) into Eq. (*A13*) gives

$$\bar{L}^3 = \frac{4{\cdot}5}{\alpha\varrho_c k_N} \, m_c^{-c} \left(\frac{k_G\beta}{3\alpha\varrho_c}\right)^{n/g} \dot{L}^{-n/g}\dot{m}_c \qquad (A14)$$

and, because of Eqs (*A6*) and (*A12*),

$$\bar{L}^{3g/n} = 3\left(\frac{4{\cdot}5}{\alpha\varrho_c k_N}\right)^{g/n} \left(\frac{k_G\beta}{3\alpha\varrho_c}\right) m_c^{1-cg/n} \, \bar{L}^{-1}\dot{m}_c^{g/n-1} \, . \qquad (A15)$$

This equation can be rewritten as

$$\bar{L}^{1+3g/n} = 3B_N m_c^{1-cg/n}\dot{m}_c^{g/n-1} \, . \qquad (A16)$$

Taking logarithms we have

$$(1 + 3g/n)\log\bar{L} = \log(3B_N m_c^{1-cg/n}) + (g/n - 1)\log\dot{m}_c \qquad (A17)$$

and for m_c = const. we obtain equation (*10*)

$$\frac{\mathrm{d}\log\bar{L}}{\mathrm{d}\log\dot{m}_c} = \frac{g/n - 1}{1 + 3g/n} \, . \qquad (A18)$$

LIST OF SYMBOLS

B_N	kinetic system constant, $m^{1+3g/n} s^{g/n-1}$
c	exponent of secondary nucleation
g	exponent of growth rate
k_G	growth rate constant, kg m^{-2} s^{-1}
k_N	nucleation rate constant, kg^{-1} s^{-1}
L	crystal size, m
$\bar{L}$	mean crystal size, m
$\dot{L}$	linear crystal growth rate, m s^{-1}
m_c	suspension density, kg hydrate/kg free water
$\dot{m}_c$	production rate of crystallizer, kg hydrate/kg free H_2O . s; s^{-1}
$M(L)$	percent oversize
$\dot{N}_N$	nucleation rate, number/kg free H_2O . s; kg^{-1} s^{-1}
n^0	population density of nuclei, number/m kg free H_2O; m^{-1} kg^{-1}
n	exponent of nucleation rate
$n(L)$	crystal population density, number/m kg free H_2O; m^{-1} kg^{-1}
$\bar{t}_l$	mean retention time, s
T	temperature, °C
T_{sat}	saturation temperature, °C
z	dimensionless crystal size
α	volume shape factor
β	surface shape factor
ϱ_c	crystal density, kg m^{-3}

REFERENCES

1. Randolph A. D., Larson M. A.: *Theory of Particulate Processes.* Academia Press, New York 1971.
2. Nývlt J., Žáček S.: Kristall und Technik, *16*, 807 (1981).
3. Žáček S., Nývlt J., Garside J., Nienow A. W.: Chem. Eng. J. *23*, 111 (1982).
4. Žáček S., Nývlt J., Mullin J. W. in the book: ***Industrial Crystallization 84,*** (S. J. Jančić and E. J. de Jong, Eds), p. 455. Elsevier Science Publishers, Amsterdam 1984.
5. Garside J., Shah M. B.: Ind. Eng. Chem., Process Des. Dev. *19*, 509 (1980).
6. Ottens E. P. K., de Jong E. J.: Ind. Eng. Chem. Fundam. *12*, 179 (1973).

Note added in proof: in Fig. 3, log $\dot{N}_N$ should be placed instead of log N_N.